J Appl Electrochem (2014) 44:849–855
DOI 10.1007/s10800-014-0693-z

RESEARCH ARTICLE

Sampling dynamics for pressurized electrochemical cells

Eric J. Dufek · Tedd E. Lister · Simon G. Stone

Received: 30 December 2013 / Accepted: 28 April 2014 / Published online: 15 May 2014

Abstract A model describing the gas distribution within a constant pressure electrolysis system and how the distribution impacts electrochemical efficiencies is presented. The primary system of interest is the generation of syngas (CO and H_2) associated with the co-electrolysis of H_2O and CO_2. The model developed for this system takes into account the primary process variables of operation including total system pressure, applied current, and the inflow of reactant gases. From these, and the chemical equilibria within the system, the impact on electrochemically generated gases is presented. Comparison of predicted and measured faradaic efficiency of an electrode's processes reveals significant disagreement under certain conditions. Methods to minimize and account for the discrepancy are presented with the goal of being able to discern, in a real-time manner, degradation of electrode performance. Comparison of the model to experimental data shows a strong correlation between the two with slight variation in experimental data, which is attributed to reversible system dynamics such as wetting of the gas diffusion electrode used as the cell cathode.

Keywords CO_2 · Electroreduction · Pressurized electrolysis · Syngas

E. J. Dufek (✉) · T. E. Lister
Idaho National Laboratory, P.O. Box 1625, Idaho Falls, ID 83415, USA
e-mail: eric.dufek@inl.gov

S. G. Stone
Giner, Inc., 89 Rumford Ave, Newton, MA 02466, USA

1 Introduction

The electroreduction of CO_2 in aqueous systems has the potential to generate a suite of products [1]. While CO_2 reduction is known to produce a multitude of different products, Ag and Au have high selectivity for CO generation and can readily be used in high surface area GDEs [2–7]. Recently, there has been significant interest in the co-electrolysis of CO_2 and H_2O using metal electrodes for the generation of CO and H_2 (syngas) [2–4, 7–15]. The utility of syngas is that once generated, it can serve as a precursor for the production of secondary chemicals. While CO_2 reduction is hindered by both kinetic and solubility issues at room temperature, key advances have been made to increase achievable current densities and to minimize the kinetic limitations including the use of optimized electrode structures [8], the use of ionic liquid mediators [16], and the use of pressurized electrolysis cells [12].

One means to increase the yields from CO_2 reduction is the use of a gas diffusion electrodes (GDE) at the cathode [2, 4, 8, 10]. When considering the co-electrolysis of CO_2 and H_2O, it is important to note that electrochemical processes can occur at both the exterior of the electrode and within the interior framework. Within the GDE interior the formation of a three phase boundary between the solid electrode surface, a thin electrolyte phase and the gaseous phase reduce the dependence of gas solubility in the electrolyte for electrochemical reactions. Pressurized systems for CO_2 reduction provide the opportunity to further increase achievable current densities due to the increased solubility of CO_2 [6, 12, 17]. To this end when combined, GDEs and elevated pressure have resulted in current densities in excess of 350 mA cm^{-2} and faradaic efficiency (FE) for CO generation greater than 80 % have been reported [12, 17].

Reduction of CO_2 in a pressurized reactor has been reported at a multitude of different electrode surfaces [6, 12, 17–22]. The use of pressurized systems for CO_2 reduction is attractive as it minimizes the pressure swings necessary when using industrial sources of CO_2 and when introducing a syngas feed into a catalysis bed for secondary product generation. While the continual operation of electrolysis systems for CO_2 reduction have shown FE in excess of 80 % for CO generation at 275 mA cm^{-2} at 24.6 atm, the systems also show alterations in product generation as experimental runs progress [12]. The variance in data makes it difficult to adequately distinguish between decreased efficiency for CO generation due to changes in the dynamics of the pressurized system, such as alterations in the partial pressure of CO_2 and electrode poisoning. The present work uses earlier studies as the foundation to develop a predictive system model which can be used to assess electrode performance in continuously operating pressurized electrolysis systems in a real-time manner. While these data are presented for the CO_2 reduction system, it is valid for other pressurized electrochemical systems which involve either reactant or product gases.

2 Experimental

All experiments were conducted using a pressurized electrolysis cell acquired from Giner, Inc.. As has been previously reported, the cell was a component in a full pressurized electrolysis system capable of independent anode and cathode pressure control [12]. Separation of the electrode compartments was achieved using a Nafion® 115 membrane. The flow frame on the cathode side of the electrolysis cell allowed CO_2 (welding grade, Norco) to be introduced to the backside of an Ag GDE (Silflon®, Gaskatel). Prior degradation studies have shown the utility of using this grade of CO_2 without significantly impacting cathode performance [9]. A porous Ag sheet (800 μm pores, Sterlitech) was used to facilitate contact between the 316 stainless steel cell frame and the GDE, while minimizing solution contact with the cell endplate. The generation of O_2 at the anode was achieved using an Ir-based dimensionally stable anode (DSA) supported on Ni mesh. The DSA was prepared in-house using a previously described method [12]. Both the anode and cathode had geometric area of 8.4 cm^2.

A key component of the pressurized electrolysis system is the pair of independent gas/liquid separators (Swagelok, 300 mL volume) located on both the cathode and anode side of the cell. These allow the product gas stream to be sampled during experiments. Including tubing, cell, and the gas/liquid separators, the total volume of the respective anode and cathode compartments was 320 mL. Two Model 81946 high pressure pumps (Micropump) equipped with variable speed controllers were used to continuously recirculate solution through the system. All experiments were conducted at a constant pressure and temperature using a 0.5 M K_2SO_4 (160 mL) and a 2.5 M KOH anolyte (120 mL). With these electrolytes, K^+ serves as the primary charge carrier from the anode to the cathode through the Nafion® 115 membrane. Both electrolyte solutions were cycled at a rate of 100 mL min^{-1}. This flow rate was found to be beneficial in reducing voltage noise and overall cell voltage, most likely due to more effective removal of gas bubbles from the electrolysis cell interior. Each side of the cell was independently pressurized using CO_2 for the cathode and Ar (for pressure balance) on the anode side. Following pressurization, a 1.25 h equilibration time was allowed to ensure that cell chemistries had stabilized prior to starting electrolysis experiments and to ensure that temperature and pressure were being adequately maintained. Cell temperature was monitored using a thermocouple imbedded in the cathode endplate. CO_2 was introduced to the electrolysis cell using a calibrated Aalborg 0–200 mL min^{-1} CO_2 mass flow controller with the pressure of the CO_2 source maintained at 6 atm above the cathode pressure to prevent backflow. Constant currents were supplied using a 35 V, 10 A DC power supply (BK Precision).

During operation, pressure on both sides of the cell was maintained using backpressure regulators and the anode pressure was maintained at approximately 75 % of the cathode pressure. Upon exit from the backpressure regulator, the cathode product gas was at ambient pressure and was passed through a chilled water trap (to condense water vapor) prior to direct introduction to a Hewlett Packard 5890 gas chromatograph (GC) which was used for gaseous product analysis as described elsewhere [2]. Sampling of the cathode product gas occurred at 10–15 min intervals and included GC analysis and measurement of product gas flow rate using an ADM 1000 digital flow meter (Agilent). The only cathode products detected were CO and H_2, although it is anticipated that trace quantities of other products were generated over the course of the experiments. The only detected anode product was O_2 indicating that no significant crossover of cathode gases occurred during the course of experiments.

3 Results and discussion

The successful pressurized electroreduction of CO_2 in a continuous, non-batch reactor setting presents issues in determining the dynamics of cell operation. In particular, how products are generated in a near real-time manner

enables a more thorough understanding of how electrode processes are evolving and if degradation in electrode performance is occurring. The present work seeks to more fully describe how the combined product and reactant gases interact with electrolyte at different pressures; and to apply this description to the development of schemes which minimize the lag between the real-time and as measured electrode processes.

Maintaining a constant pressure in a fixed volume electrolysis cell requires that the gases entering and exiting the system will be monitored and adjusted. In systems where gases are both reactants and products such as the aqueous electroreduction CO_2 to syngas, a lag time between product generation and sampling is created. This lag is partially governed by the partial pressure changes that occur as gases are introduced or generated, which can be correlated to flow and current parameters. The system volume composition at any one time is complicated by the solubility of gases, which is dictated by their respective partial pressures as defined by Henry's law.

In the case of the electroreduction of CO_2, the efficiency of CO generation is dictated by the pressure of CO_2 (P_{CO_2}) present in the system [6, 12]. However, as CO and H_2 (from H_2O reduction) are generated in the fixed volume, constant total pressure (P_{total}) system, P_{CO_2} must decrease to account for the electrochemically generated gas. As such, the pressure-dependent voltage efficiency for the reduction of CO_2 is impacted. To obtain a better grasp of how the sampled product stream relates to the actual electrode processes, and to gage if changes in gas distribution are related to pressure differences or changes in electrode activity, an in-depth understanding of how the various process variables impact effluent gas is needed.

Recall that the present electrolysis system volume contains both free volume occupied by the gaseous components in the system, and volume occupied by aqueous electrolyte which is continuously circulating through the system. Based on the system configuration, the gas volume for the cathode side of the cell was 160 mL. Using this volume and the ideal gas law, it becomes possible to determine the total moles of gas present in the system at each temperature and pressure condition. During constant temperature and pressure operation, this value serves as the bound which dictates the quantity of gas which must be released from the pressurized system through either conversion to soluble products or by exiting through the pressure regulator. It should be noted that for the present work, a constant temperature of 60 °C was used for both calculation and experiments. The temperature was verified using a thermocouple which was embedded on the cathode side of the electrolysis cell. The elevated temperature was chosen to enhance cell efficiency based on previous reports [2, 12].

Using the total gas volume, the variable gas composition can be determined given the electrochemical and chemical bounds of the system. Electrochemically, the reduction of CO_2 to CO and the reduction of H_2O to H_2 (Eqs. 1 and 2, respectively) are the two major reactions in neutral and basic conditions. In acidic conditions, Eqs. 3 and 4 predominate. For the sake of simplicity, the following discussion will focus on the neutral and basic conditions which existed for the present experimental work, but highlight where differences in implementation of the model would be necessary for acidic conditions.

$$CO_2 + H_2O + 2e^- \rightarrow CO + 2OH^- \qquad E^0 = -0.932 \text{ V} \tag{1}$$

$$2H_2O + 2e^- \rightarrow H_2 + 2OH^- \qquad E^0 = -0.828 \text{ V} \tag{2}$$

$$CO_2 + 2H^+ + 2e^- \rightarrow CO + H_2O \qquad E^0 = -0.104 \text{ V} \tag{3}$$

$$2H^+ + 2e^- \rightarrow H_2 \qquad E^0 = 0 \text{ V} \tag{4}$$

For the present work, it is assumed that, while some minor products may be generated from CO_2 reduction [23], the total efficiency associated with these trace products is minimal. This assumption is supported by prior work using Ag-based systems, which show little if any non-CO products for CO_2 reduction [2, 4].

For each of the respective electrochemically generated products, the moles generated (dm) over a given amount of time (dt) can be defined using Eq. 5 where i is the applied current,

$$dm = idt(\text{FE})(nF)^{-1} \tag{5}$$

FE is the faradaic efficiency for the respective process at a given reactant gas partial pressure (P_{CO_2}), F is Faraday's constant (96,485 C mol^{-1} electrons), and n is the electrons involved in the respective electrochemical process. Due to the dependence of this mole rate on P_{CO_2}, which changes during cell operation, it is necessary to perform measurements early in an experimental run across the relevant range of pressures. To accomplish this, data were collected at points between 10 and 15 min after starting electrolysis at various pressures. While sampling at an earlier point in the experiment would have been ideal, volume and sampling constraints stemming from the GC purging requirements and the pressurized systems restricted the interval for reproducible samples to a minimum of 10 min. Due to this lag, the measured FE is denoted as FE*, while the theoretical efficiency based on the real-time electrode processes is FE. The FE* data for CO generation (FE^*_{CO}), which are a combination of previously reported points [12] and new experimental data across a range of CO_2 pressures, provide a basis by which the pressure dependence of

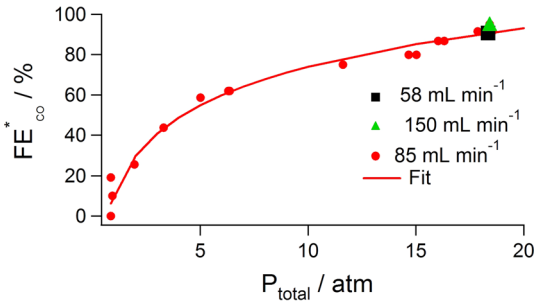

Fig. 1 Experimental data and fit for operation of the pressurized electrolysis cell at 225 mA cm^{-2} at a υ_{CO_2} of 58, 85, or 150 mL min^{-1}. Experimental data points were collected within the first 15 min of cell operation to minimize any possible deviation associated with a decrease of P_{CO_2} during cell operation

FE_{CO} can be determined (Fig. 1). At the highest pressures investigated, multiple CO_2 flow rates (υ_{CO_2}) were used to verify that flow rate was not impacting the initial data point. As will be pointed out below, υ_{CO_2} has a distinct impact on extended cell operation.

In addition to electrochemically generated products, attention needs to be paid to the chemistry of the system. Both the generation of H_2 and CO (Eqs. 1, 2) in neutral and basic conditions result in the production of OH^- for the present system. This, in turn, reacts readily with CO_2 to form either carbonate or bicarbonate (Eqs. 6, 7, and 8).

$$CO_2 + H_2O \rightleftharpoons H_2CO_3 \tag{6}$$

$$H_2CO_3 + OH^- \rightleftharpoons HCO_3^- + H_2O \qquad pK_a 6.35 \tag{7}$$

$$HCO_3^- + OH^- \rightleftharpoons CO_3^{2-} + H_2O \qquad pK_a 10.33 \tag{8}$$

Due to the pre-equilibration step (1.25 h after pressurization prior to starting experimentation), it can be assumed that the carbonate chemistry is fully equilibrated prior to the start of experimentation and, therefore, any changes with respect to the carbonate equilibria will be based on the electrochemically generated OH^-. For the calculations described below, it was also assumed that the primary carbonate in solution was HCO_3^-. Measurement of the pH at the completion of multiple experiments conducted at different pressures and temperatures showed a maximum pH of 7.63 at a CO_2 flow rate of 85 mL min^{-1} which supports this assumption.

In order to maintain constant pressure during operation of a fixed system volume, gas must be either released from the system or chemically converted to a non-gaseous product. Due to the continually flowing nature of the electrolysis cell, it can be assumed that effective mixing of the three gases occurs within the cell, thus the gas exiting the system is truly representative of the combined product and reactant gases. The respective mole content and subsequently the partial pressure of each of the three primary gases (CO_2, CO, and H_2) can be defined by a set of equations. First is the experimentally determined FE_{CO} (Eq. 9, fit to data shown in Fig. 1) which can be substituted into Eq. 5 above.

$$FE_{CO} = 27.6 \ln P_{CO_2} + 10.4 \tag{9}$$

Ignoring competing processes (i.e., trace production generation), FE_{H_2} is then defined using Eq. 10. Using this value in Eq. 5 provides the mole H_2 generated.

$$FE_{H_2} = 1 - FE_{CO} \tag{10}$$

For a given time period or step, the nature of the moles of CO_2 (m_{CO_2}) present in the system can be defined as

$$m_{CO_2} = m_{CO_2,ini} - m_{CO} + m_{CO_2,entering} - m_{CO_2,leaving} - 2(m_{CO} + m_{H_2}), \tag{11}$$

where $m_{CO_2,entering}$ and $m_{CO_2,leaving}$ are defined by the respective flow rates of gas entering (υ_{CO_2}) and leaving the system ($\upsilon_{CO_2,leaving}$). Due to the assumption of uniform mixing of the gases in the electrolysis system, the $m_{CO_2,leaving}$ is dictated by the mole fraction of CO_2 necessary to maintain a constant pressure. Additionally, the molar quantity of CO_2 which is converted to CO (m_{CO}), and the quantity converted to HCO_3^- due to electrochemically generated OH^- per Eqs. 1, 2, 5, and 7 are all taken into account. Using the mole quantities for CO_2, CO, and H_2 (the three gaseous products), the mole fraction and subsequently the P_{CO_2}, P_{CO}, and P_{H_2} can be readily obtained given that P_{total} and the system volume are known. For the present work, the above set of equations can be converted into an analytical solution such that an iterative calculation with a time step of 60 s is used to determine the various gas quantities and their respective mole fraction and partial pressures (P_{CO_2}, P_{CO} and P_{H_2}).

It should be noted that as written, Eq. 11 only holds for the electrochemical generation of CO and H_2 in neutral and slightly basic conditions. If the system chemistry was to change and an acidic catholyte was to be used, or should the system rely on the transfer of H^+ from an anode reaction, then modifications are needed. For an acidic catholyte and the transfer of H^+ from the anode, the last two terms (m_{CO} and m_{H_2}), which are related to carbonate equilibrium in Eqs. 6–8, become unnecessary as the respective electrochemical reactions in Eqn. 3 and 4 do not generate OH^-. In this instance, few other modifications are needed as the H^+ consumed at the cathode would match the H^+ transferred from the anode. This situation would result in the subsequent change in P_{CO_2} being lessened. Should a non-H^+ cation serve as the charge carrier from the anode (i.e., an acidic catholyte and K^+ transferred from the anode) then a hybrid model based on the evolution of pH would be necessary. The hybrid model would transition from not including the m_{CO} and m_{H_2} terms to including them as H^+ is consumed. The third possibility where H^+

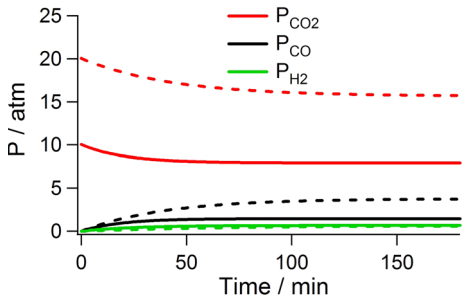

Fig. 2 The predicted impact on P_{CO_2}, P_{CO}, and P_{H_2} as the total pressure of the electrolysis system is altered from 10 to 20 atm. υ_{CO_2} 85 mL min^{-1}, i 1.9 A (225 mA cm^{-2})

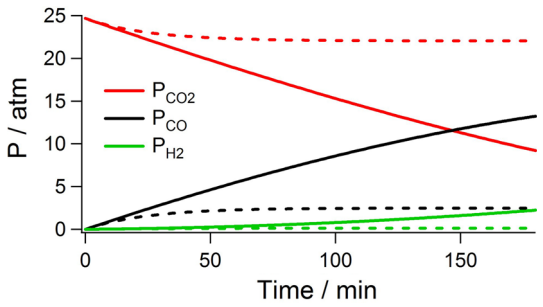

Fig. 3 The predicted impact on P_{CO_2}, P_{CO}, and P_{H_2} as the υ_{CO_2} of the electrolysis system is altered from 50 to 150 mL min^{-1}. P_{total} 25 atm, i 1.9 A (225 mA cm^{-2})

becomes important is the use of a neutral electrolyte and the transfer of H^+ from the anode. This scenario is a bit more difficult in a non-equilibrium condition as the H^+ can react with both carbonate species and OH^-. However, equilibration results in the balancing of the OH^- generated electrochemically and the H^+ transferred from the anode removing the need for the m_{CO} and m_{H_2} terms. One other note regarding the use of an acidic catholyte is the need to minimize wetting of the GDE which becomes important as the production of H_2 is more favored than CO. Thus said, effective management of the GDE still allows generation of appreciable levels of CO as was recently discussed for a system generating Cl_2 and syngas from a system using HCl as both the catholyte and anolyte at ambient pressure [11].

During extended operation of the pressurized system there are three primary process variables which can be manipulated to impact product distribution: P_{total}, υ_{CO_2}, and i, Converting each of the molar quantities from the equations above into partial pressures using the ideal gas law provides insight into how each of the process variables impacts product distribution. These data are shown in Figs. 2, 3, 4. While similar changes can be imparted by altering more than one of the variables, the impact on other metrics, such as cell energy efficiency (ε) which is related to the cell voltage, enthalpies of formation and FE, and total product generation, must also be taken into account. As an example, from previously reported data, the ε drops from 55 to 32 % as the current density is increased from 118 to 350 mA cm^{-2} despite only a minor change in FE_{CO} [12]. Adjusting υ_{CO_2} provides the most straight forward way to maintain cell conditions near their original starting conditions thus providing more opportunity to gage how the two other process variables, particularly i, are impacting overall cell performance. Altering υ_{CO_2} has not been found to impact the cell voltage and hence ε [12]. Likewise, adjusting the total system pressure has a profound impact on the quantity of CO generated but with little impact on ε.

During operation of electrolysis cells, it is important to follow product generation to identify how electrode

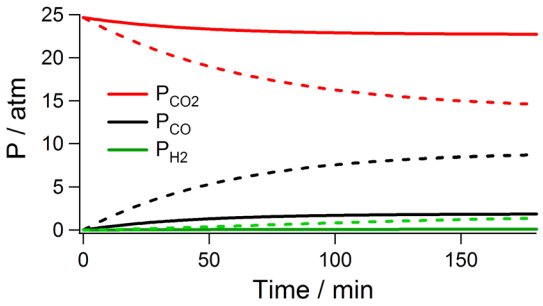

Fig. 4 The predicted impact on P_{CO_2}, P_{CO}, and P_{H_2} as the i of the electrolysis system is altered from 0.85 A (100 mA cm^{-2}) to 2.95 A (350 mA cm^{-2}). υ_{CO_2} 85 mL min^{-1}, P_{total} 25 atm

processes evolve and to gauge any potential poisoning of the electrode. In ambient pressure cells, comparing consecutive data points provides a straight-forward manner of this evaluation. However, as highlighted in Figs. 2, 3, 4, and in Eq. 9, in pressurized systems, the comparison and the ability to gauge changes in electrode processes in a real-time manner become more problematic. Using the data generated from Eqs. 9–11, along with the initial data presented in Fig. 1, and holding i and P_{total} constant, while varying υ_{CO_2}, it is possible to calculate both the expected, sampled experimental faradaic efficiency (FE*) and the FE of the real-time electrode processes. As shown in Figs. 2, 3, 4 the dynamic nature of the electrochemical and chemical processes impacts both FE and FE* as the electrolysis cell is continually operated. It should be noted that FE is closely associated with the P_{CO_2} and FE* is more closely tied to the combined mole fraction of the gases in the electrolysis system as dictated by all the chemical and electrochemical mechanisms described above. Thus, for the two to be in relatively close agreement, a sufficiently high υ_{CO_2} is necessary to minimize the overall drop in P_{CO_2} (as dictated by Eq. 11). The elevated flow rates also shorten the time to fully purge the analysis system and may decrease time required to achieve system equilibration. Figure 5 highlights the predicted difference in FE′ and

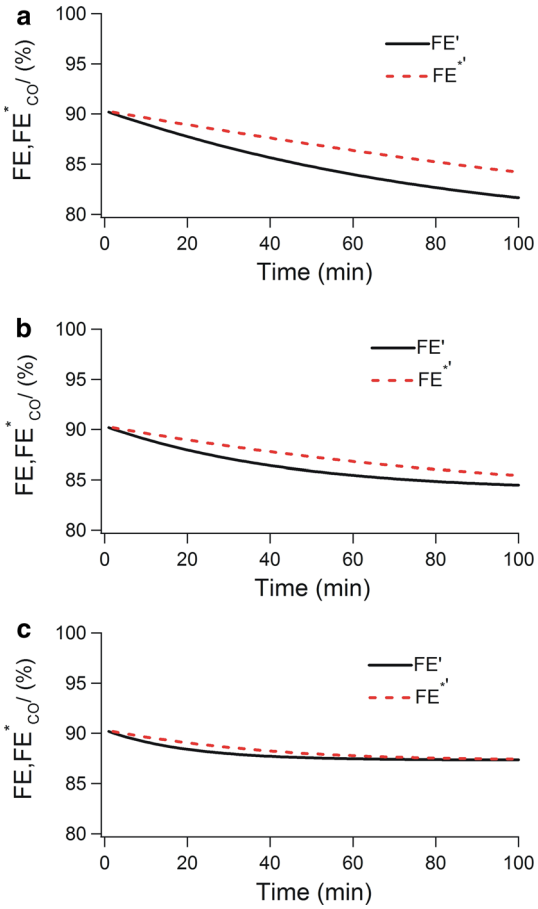

Fig. 5 Comparison of predicted values of FE′ and FE*′ for CO production based on P_{CO_2} decreases during cell operation at 18.5 atm. The prime indicates that the values are calculated predictions and not experimentally obtained values. Predictions were based on Eq. 11 and experimental data in Fig. 1. υ_{CO_2}: **a** 60 mL min^{-1}, **b** 85 mL min^{-1} and **c** 150 mL min^{-1}

FE*′ (where the prime denotes that the value is calculated) using the equations above at a commercially viable current of 1.9 A (225 mA cm^{-2}) and a system pressure of 18.5 atm for three different υ_{CO_2}. Of note is that the variance between FE and FE* for CO is less than 1 % when υ_{CO_2} is increased to 150 mL min^{-1}.

From Fig. 5, it becomes clear that to most effectively identify degradation processes which occur during cell operation either high υ_{CO_2} is necessary or a full suite of data similar to Fig. 1 are required for each *i*. A key concern when relying on high υ_{CO_2} is that the products in the gas stream (CO and H_2) become diluted due to the high quantities of CO_2 introduced into the system. For this reason, validation of the model was performed, while operating the cell at 225 mA cm^{-2} with a υ_{CO_2} of 85 mL min^{-1} to correspond with the data in Fig. 1. Three independent experiments were performed over 2 days to gauge the applicability of the present model, and to interpret if variance within the individual experiments impacted

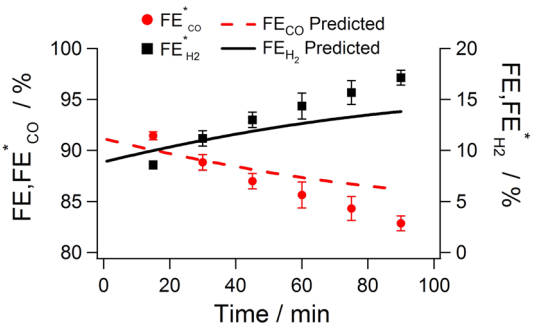

Fig. 6 Comparison of the predicted model and the average FE^*_{CO} and $FE^*_{H_2}$ of three independent experiments at 225 mA cm^{-2}, υ_{CO_2} = 85 mL min^{-1}, P_{total} = 18.5 atm

future cell performance as would be expected from irreversible electrode poisoning. These data are presented in Fig. 6. For the three experiments, the cell configuration was maintained and the same anode and cathode were used for each run. The electrolyte was exchanged between runs and the system was fully depressurized and brought to ambient temperature between experiments. Prior to the start of each run, the system was repressurized and heated as described in the experimental section.

From Fig. 6, it is evident that the model developed for determining how changes in P_{CO_2} impact both FE_{CO} and FE_{H_2} closely follows experimental conditions. During operation, the overall cell voltage for each of the three runs gradually decreased from ~3.6 to 3.4 V. This closely mimics data acquired at the same current density but using an υ_{CO_2} of 150 mL min^{-1} [12]. The data also suggest that during cell operation the overall dynamics start to vary from the bounds of the model as the experimentally obtained FE^*_{CO} drops below the model prediction and the $FE^*_{H_2}$ increases above predicted values. Similar behavior where the FE_{CO} decreases and FE_{H_2} increases has been reported for ambient pressure systems over extended operation [2, 7]. However, as with the ambient pressure investigations, the run-to-run repeatability is high with efficiencies in excess of 90 % at the initiation of each independent trial. Thus, the most likely cause of the decrease in CO generation efficiency is an alteration of the electrode such as the wetting of the GDE, which would increase H_2 generation as is observed in the data, rather than the electrochemical processes which impact the partial pressures of the gases within the system.

4 Conclusions

A model for determining the dynamics within a constant pressure, extended operation electrolysis system is presented. The primary impetus for the work was the ability to gauge in a real-time manner if electrode processes were

changing due to poisoning or other degradation mechanisms. A key component of sufficiently describing systems which both consume and generate gas is that the impact of variable partial pressures be taken into account. For the present work, the three main process variables which have been found to impact the efficiency of the electrochemical process are υ_{CO_2}, i, and P_{total}. A strong correlation between the developed model and actual data suggests that the model adequately describes pressurized systems for the generation of syngas from the coreduction of CO_2 and H_2O. Slight variations in the experimental data from the model as experiments progressed indicate that reversible changes occur in the system most likely attributed to progressively more wetting of the GDE as the experiments progressed.

Acknowledgements Work supported through the INL Laboratory Directed Research and Development (LDRD) Program under DOE Idaho Operations Office. This manuscript has been authored by Battelle Energy Alliance, LLC under Contract No. DE-AC07-05ID14517 with the U.S. Department of Energy. The United States Government retains and the publisher, by accepting the article for publication, acknowledges that the United States Government retains a non-exclusive, paid-up, irrevocable, world-wide license to publish or reproduce the published form of this manuscript, or allow others to do so, for United States Government purposes.

References

1. Whipple DT, Kenis PJA (2010) Prospects of CO(2) utilization via direct heterogeneous electrochemical reduction. J Phys Chem Lett 1:3451–3458
2. Dufek EJ, Lister TE, McIlwain ME (2011) Bench-scale electrochemical system for generation of CO and syn-gas. JAppl Electrochem 41:623–631
3. Delacourt C, Ridgway PL, Newman J (2010) Mathematical modeling of CO2 reduction to CO in aqueous electrolytes. I. Kinetic study on planar silver and gold electrodes. J Electrochem Soc 157:B1902–B1910
4. Delacourt C, Ridgway PL, Kerr JB, Newman J (2008) Design of an electrochemical cell making syngas ($CO + H_2$) from CO_2 and H_2O reduction at room temperature. J Electrochem Soc 155:B42–B49
5. Hori Y, Wakebe T, Tsukamoto T, Koga O (1994) Electrocatalytic process of coselectivity in electrochemical reudction of CO_2 at metal-electrodes in aqueous-media. Electrochim Acta 39:1833–1839
6. Hara K, Kudo A, Sakata T (1995) Electrochemical reduction of carbon-dioxide under high-pressure on various electrodes in an aqueous-electrolyte. J Electroanal Chem 391:141–147
7. Dufek EJ, Lister TE, McIlwain ME (2012) Influence of electrolytes and membranes on cell operation for syn-gas production. Electrochem Solid State Lett 15:B48–B50
8. Jhong HR, Brushett FR, Kenis PJA (2013) The effects of catalyst layer deposition methodology on electrode performance. Adv Energy Mater 3:589–599
9. Dufek EJ, Lister TE, McIlwain ME (2011) Influence of S contamination on CO(2) reduction at Ag electrodes. J Electrochem Soc 158:B1384–B1390
10. Delacourt C, Newman J (2010) Mathematical modeling of CO_2 reduction to CO in aqueous electrolytes. II. Study of an electrolysis cell making syngas ($CO + H_2$) from CO_2 and H_2O reduction at room temperature. J Electrochem Soc 157(B1911):B1926
11. Lister TE, Dufek EJ (2013) Chlor-syngas: coupling of electrochemical technologies for production of commodity chemicals. Energy Fuel 27(4244):4249
12. Dufek EJ, Lister TE, McIlwain ME (2012) Operation of a pressurized system for continuous reduction of CO_2. J Electrochem Soc 159:F514–F517
13. Whipple DT, Finke EC, Kenis PJA (2010) Microfluidic reactor for the electrochemical reduction of carbon dioxide: the effect of pH. Electrochem Solid State Lett 13:B109–B111
14. Thorson MR, Siil KI, Kenis PJA (2013) Effect of cations on the electrochemical conversion of CO_2 to CO. J Electrochem Soc 160:F69–F74
15. Wu JJ, Risalvato FG, Sharma PP, Pellechia PJ, Ke FS, Zhou XD (2013) Electrochemical reduction of carbon dioxide. II. Design, assembly, and performance of low temperature full electrochemical cells. J Electrochem Soc 160(F953):F957
16. Rosen BA, Salehi-Khojin A, Thorson MR et al (2011) Ionic liquid-mediated selective conversion of CO_2 to CO at low overpotentials. Science 334:643–644
17. Hara K, Sakata T (1997) Large current density CO_2 reduction under high pressure using gas diffusion electrodes. B Chem Soc Jpn 70:571–576
18. Hara K, Kudo A, Sakata T (1994) Electrochemical CO_2 reduction on a glassy carbon electrode under high pressure. J Electroanal Chem 421:1–4
19. Hara K, Tsuneto A, Kudo A, Sakata T (1994) Electrochemical reduction of CO_2 on a Cu electrode under high-pressure—factors that determine the product selectivity. J Electrochem Soc 141:2097–2103
20. Kudo S, Nakagawa S, Tsuneto A, Sakata T (1993) Electrochemical reduction of high-pressure CO_2 on Ni electrodes. J Electrochem Soc 140:1541–1545
21. Nakagawa S, Kudo A, Azuma M, Sakata T (1991) Effect of pressure on the electrochemical reduction of CO_2 on group-VIII metal-electrodes. J Electroanal Chem 308:339–343
22. Vassiliev YB, Bagotzky VS, Osetrova NV, Khazova A, Mayorova NA (1985) Electroreduction of carbon-dioxide. 1. The mechanism and kinetics of electroreduction of CO2 in aqueous-solutions on metals with high and moderate hydrogen overvoltages. J Electroanal Chem 189:271–294
23. Kuhl KP, Cave ER, Abram DN, Jaramillo TF (2012) New insights into the electrochemical reduction of carbon dioxide on metallic copper surfaces. Energy Environ Sci 5:7050–7059